AEGC2019 Data to Discovery
Australasian Exploration Geoscience Conference 2-5 September 2019 • Perth, Western Australia
Incorporating the AIG, ASEG, PESA, and WABS

Magnetic Field Inversion – the cost of freedom

Leonardo B. Vital
Observatorio Nacional and CSIRO Mineral Resources North Ryde, Sydney
leobvital@gmail.com, Leonardo.Beserravital@csiro.au

Clive Foss
CSIRO Mineral Resources North Ryde, Sydney
clive.foss@csiro.au

Vanderlei C. Oliveira Jr
Observatório Nacional Rio de Janeiro, Brazil
vandscoelho@gmail.com
vanderlei@on.br

Valeria C. F. Barbosa
Observatório Nacional Rio de Janeiro, Brazil
valeria.valcris@gmail.com, valcris@on.br

SUMMARY

We created a funnel-shaped magnetic body from magnetite powder dispersed in plaster and used a travelling 3-component fluxgate magnetometer to map the magnetic field at a low elevation above it. This provided a dataset with signal and noise characteristics similar to those of a field survey, but for a source much better known than any buried geological body. We then used this survey data and the known source details to evaluate recovery of that information from inversions with different degrees of freedom and constraint. This provides guidance in evaluation of inversion results from field data for which the source characteristics are unknown.

We found that because of small imperfections in the data and model, the inversion result closest to the truth, although fitting the data quite acceptably, is not the model with the smallest data misfit. Chasing further reduction in data misfit in some cases leads to inversion results which better fit the data but which diverge from the known magnetization. Furthermore, inversions to fit the noise-free field forward computed from a digital version of the model do not recover that exact model, with increasing deviation (but smaller data misfits) as increasing complexity is added to the inversion models.

Key words: magnetic field parametric inversion.

INTRODUCTION

Magnetic field inversions are generally run with the primary objective of gaining an insight into subsurface geology. However, the primary objective of the inversion algorithm is principally to minimise data misfit. Inversion model results are commonly used without consideration of this disconnect and may be readily accepted as reliable representations of the subsurface, even by those aware of the caveats of non-uniqueness in solution of the inverse problem. There is a psychological implication that a model closely matching the data has validity, particularly if that match is presented graphically as a pair of near-identical images. Inversions with greater degrees of freedom naturally have increased capability to match data, but the question has to be asked whether or not a specific increase in freedom improves or detracts from the quality of the resulting inversion model as a prediction of the subsurface. To investigate the predictive capability of inversion software used in geological investigations we have generated a magnetic field data-set from a magnetization much better known than geological subsurface magnetizations which are invariably under-sampled. Such tests are usually performed virtually using forward computed data with added noise of specified characteristics. In this study we built a funnel-shaped magnetic model and measured the magnetic field above it, to provide a dataset with signal and noise similar to those measured in a geophysical field survey. We then inverted the data using two different parametric inversion softwares to investigate reliability or otherwise in recovering details of the known source.

We do not here consider the initial and fundamental question of whether a specific anomaly can be recognised as being due to a funnel-type geometry, thereby pre-qualifying the selection of this model type. Nor do we consider the supplementary question of how the best selected funnel model compares to competitive models of other geometries. For any discrete anomaly there will be a best-fitting funnel model or suite of funnel models, and if those models are deemed to be realistic according to whatever known or expected constraints are available, then acceptance or rejection of the models according to their compatibility with measured magnetic field data is an interpretive decision. Furthermore, if some grounds for discrimination are available, the preferred model need not be that which has the smallest data misfit.

We do not here test a voxel inversion. Issues of freedom and non-uniqueness are even more relevant for voxel inversion models which have greater variability than corresponding parametric models, presenting different property values for multiple volume subsets of the ground. Many geologists prefer these models as they suggest irregular geometries and variable property distribution as may be expected of geology. However, it is specifically this apparent level of detail that is the weakest and least justified aspect of those models. It is very difficult to assess whether a voxel model with greater degrees of freedom and variability, or a parametric model of (in many cases synthetic) simplicity provide the better insight to and closer representation of the subsurface. This question needs to be considered on a case by case basis as some subsurface geologies may be better suited to voxel inversion and others better suited to parametric inversion. The question also depends on what is required of the inversion. For instance, if depth to the top of a magnetization is required, that is better supplied by a parametric inversion because depth estimation requires a source shape assumption or specification. We intend to extend our study to include voxel inversion at a later date.

Some parametric and voxel inversion algorithms step between models to explore the multi-dimensional model space. Parametric inversion is generally better suited to such investigations, as repeat inversions following stepwise variation of a selected parameter establish sensitivity of the model to that parameter, and map co-dependence between parameters. Model-stepping for voxel models is generally only effective in exploration of a local zone of the model space, as it is difficult to step between disconnected regions in model space that may also be feasible. Furthermore, presentation of many voxel model solutions generally requires that they be amalgamated in some way, which may be little more informative than presentation of a single model.

It is likely that an individual inversion problem has an optimum degree of freedom for any particular inversion algorithm, dependant on the data (including any independent constraints), the 'truth' of the property distribution in the subsurface, and what is required in interrogation of the subsurface by the inversion. However, as the critical factor of the actual subsurface property distribution is unknown, we cannot confidently pre-select the optimum degree of freedom for an inversion. The general penalty for allowing an inversion insufficient freedom is an oversimplification and thereby possibly a gross misrepresentation of the subsurface. Increase in the degree of freedom of an inversion might be thought to progressively allow closer approximation to the ground truth, but unfortunately the common penalty for allowing an inversion too great a freedom is embellishment and thereby possibly just as great a misrepresentation of the subsurface. The optimum degree of freedom for an inversion (although we are unable to know it) is that for which both decrease and increase in degree of freedom lead to progressively less satisfactory representations of the subsurface.

MAGNETIZATION MODEL AND SURVEY DETAILS

A tapered circular pipe is a model occasionally used to represent a geological body, in particular kimberlite pipes.

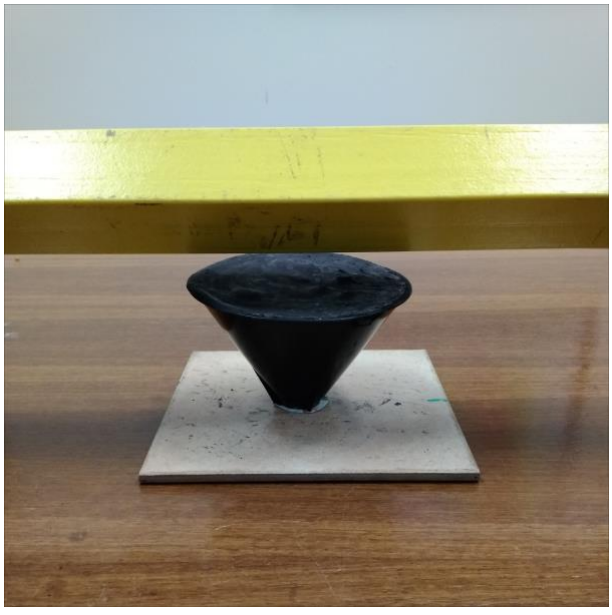

Figure 1. The funnel model placed beneath the track along which the 3 component magnetometer travels.

We constructed a funnel-shaped model and placed it beneath a track along which a 3-component fluxgate was drawn (Figure 1). The fluxgate sensors are concealed within a block, and the block is concealed within the track, so we could only imperfectly locate the sensors relative to the model. The model was moved in steps perpendicular to the track across a flat surface, and at each step a new 'flight-line' of data was acquired. This method of survey acquisition minimised re-orientation of the sensor between flight-lines. The background field is separated by subtraction of the field measured with the model removed. The resulting TMI map is shown in Figure 2.

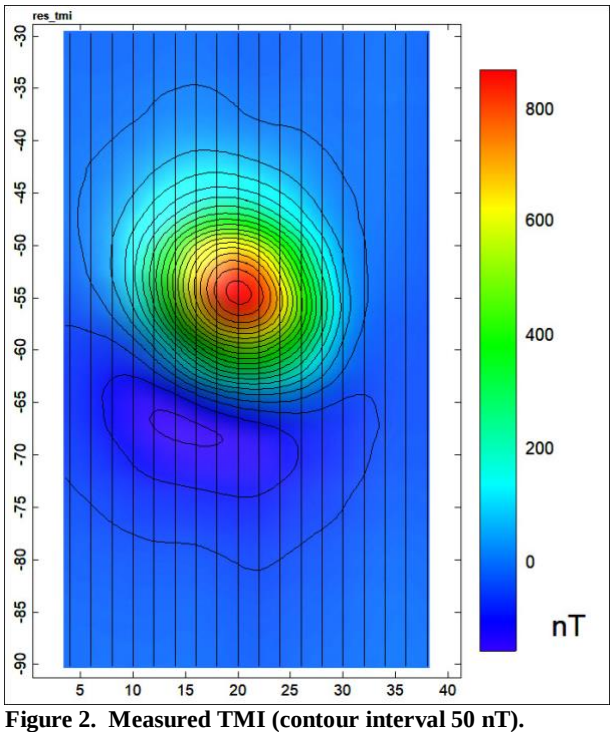

Figure 2. Measured TMI (contour interval 50 nT).

INVERSION RESULTS USING MODELVISION

Modelvision™ (Pratt et al., 2005) is a parametric modelling and inversion package. Of the two inversion methodologies available in ModelVision we used the simple Marquardt ridge-regression inversion (Marquadt, 1970). The sole objective of this inversion is to reduce the rms data misfit. The inversion algorithm includes a stepping function which allows a closer focus on model space as a data-misfit reduction is found, or a wider focus if no reduction is found (to escape from local minima). The inversion progresses step by step towards a requested misfit target, and inversion can be interspersed with forward modelling for user-guided inversion. Most importantly, individual parameters can be set free or fixed in an inversion, and minima and maxima can be set for the permitted values of each parameter.

Models are built from combination of individual bodies of various type. Each body has homogeneous properties, and in few cases do bodies have enforced linkage to each other. The intent is primarily to represent discrete distributions of property different to background which cause local variations in the gravity or magnetic fields. For this study the ground consists of a binary distribution of (near-homogeneous) magnetization within the circular funnel, and no magnetization outside it. Modelvision includes a circular funnel body ideal for this

representation. We used a model body of this type and with the known location and geometry to best-fit the measured data (an inversion of only the magnetic susceptibility value). The model (Model A) is shown in Figure 3 and its parameters are listed in Table 1. The data misfit (with a value of 10.5%) is due to imperfections in the model and mostly in data acquisition, but we are confident that the model is a close representation of the true distribution of magnetization. Many inversions of field data have similar or lower data misfit values. We repeated inversions with progressively more complex models of a circular (Model B) and polygonal (Model C) funnels with free cross-section, magnetic susceptibility, depth extent and plunge. The data misfit reduces to 9.2 and 5.3% respectively, but these models are clearly progressively poorer representations of the known magnetization distribution. In particular the models very poorly represent the deeper magnetization, which because of the increased depth and volume reduction by taper contributes very little to the anomaly, and is thereby poorly constrained.

To isolate ambiguity of inversion from data imperfection effects we forward computed the field from Model A and ran inversions of that field data. Models D and E (Figure 3 and table 1) are inversions of the Model A field using vertical circular funnel models with magnetic susceptibility values 50 and 200% of the original. The data misfits are small (1.8% and 0.6%). This low sensitivity to magnetic susceptibility is due to the tapered top edge of the source model, which facilitates change in depth (-27% to +17%) and of depth extent (+122% to -57%) to help compensate for the enforced susceptibility changes (a vertical cylinder has higher sensitivity to its magnetic susceptibility value, depth and depth extent). Such small data misfits can easily be accommodated within the larger data misfits of matching measured data, and so for this model geometry, there is an inherently low sensitivity to magnetic susceptibility and depth to the top of the magnetization.

We also inverted the Model A field data with more complex models of plunging elliptic (Model F) and polygonal (Model G) funnels using poor starting models. These models achieved small data misfits (5.0% and 2.8%) before stalling in local minima. The models are only marginally better representations of the known magnetization distribution than are the corresponding models B and C derived from the measured data. This reveals that for our measured data the fundamental ambiguity of inversion is more significant than the additional uncertainty resulting from imperfection of the data. For all inversion models estimates of depth to top and total magnetization (magnetic moment) are intrinsically more reliable than the magnetic susceptibility, top area, volume and depth extent values.

INVERSION RESULTS USING A NEW METHOD

We also present a second method for inverting magnetic data to estimate the geometry of a 3D source. This method assumes that both the magnetization vector and the depth to the top of the source are known. We approximate the shape of the geological source by an ensemble of vertically juxtaposed 3D right prisms. Each prism has a known homogeneous magnetization and a horizontal cross-section described by an unknown polygon. The vertices of the polygons approximate the horizontal depth slices of the source retrieving its geometry. The effect of the ensemble of polygonal prisms is computed based on the formulas proposed by Plouff (1976). We calculate the effect by using the Python package Fatiando a Terra (Uieda et al., 2013).

This method is an extension for magnetic data of those presented by Oliveira Jr et al. (2011) and Oliveira Jr and Barbosa (2013) for inversion of gravity and gravity-gradient data, respectively. However, differently from those authors, we also estimate the thickness of all prisms. The method also estimates the horizontal coordinates of the vertices defining the interpretation model. The method is formulated in the space domain, as a constrained nonlinear inversion. To estimate a stable solution, we introduced constraints on the geometry of the source. We use the Marquardt method to minimize the objective function introducing inequality constraints by using a strategy similar to that presented by Barbosa et al. (1999). Our method imposes seven constraints on the shape of the estimated source. Most of these constraints are defined by using the Tikhonov regularization functions of orders zero and one, by following the same approach presented by Oliveira Jr et al. (2011). Additionally, we impose here a constraint on the thickness of all prisms.

We applied our method on the measured data produced by the funnel model using an initial guess with 9 prisms, each one with 20 vertices, depth to the top 6 cm, thickness 1 cm, and all radii are equal to 7 cm, and magnetic susceptibility 0.2 S.I. We assumed that the source has an induced magnetization with inclination -61.3º and declination 4.8º, parallel to the Earth's local main field. Figure 4 shows the inverse models listed in Table 1 comparing them to the geometry of Model A. For the Model A field the estimated sources (models H and I) do not match perfectly the true source but it has a funnel-like geometry (Figures 4a and 4b). However, the misfit for model H decreases 5% and the misfit for model I increases 21% compared to Model A misfit. Inverting the computed data from Model A, we have obtained a geometry closer to the true model. Figures 4c and 4d show that the models J and K (red prisms) almost retrieve the true geometry of the source with misfits 70% and 10%, respectively, smaller than the Model A misfit. We tested a deeper depth to the top for the models I and K almost 8% deeper than Model A. For both models the misfit increases and the depth extent becomes shallower.

CONCLUSIONS

We built a simple model with relatively well-known distribution of magnetization. Inversion with the only significant unknown of magnetization (magnetic susceptibility) free, produced a model with an acceptable match to the measured data. Inversion of the field forward computed from this 'true' model using an independent software, and again with some key parameters fixed (depth to top and magnetization) produced a close but imperfect recovery of that model despite variation in the geometries used by the two softwares. With either software, increasing the freedoms for inversion progressively reduces data misfit but also leads to models progressively different to the known model. Freedom of each parameter, and freedom of different combinations of parameters, influences the inversion results differently. As the freedoms of inversion are increased, imperfection in recovering source information becomes progressively less dependent on imperfections in the data, and increasingly more dependent on compensation in any one parameter for errors in others. Consistency of this behaviour between the two independent inversion softwares emphasises that this is an inherent issue of inversion, with little dependence on the specific software used.

ACKNOWLEDGMENTS

This work was conducted during a scholarship supported by the International Cooperation Program CAPES/COFECUB at the Observatório Nacional. Financed by CAPES – Brazilian Federal Agency for Support and Evaluation of Graduate Education within the Ministry of Education of Brazil. V.C.F. Barbosa was supported by fellowships from: CNPQ (grant 307135/2014-4) and FAPERJ (grant E-26/203.091/2016). V.C. Oliveira Jr was supported by fellowships from: CNPQ (grant 308945/2017-4) and FAPERJ (grant E-26/202.729/2018). The authors thank CPRM for permission to use the aeromagnetic data set.

REFERENCES

Barbosa, V. C. F., J. B. C. Silva, and W. E. Medeiros, 1999, Gravity inversion of a discontinuous relief stabilized by weighted smoothness constraints on depth: *Geophysics*, 64, no. 5, 1429–1437.

Marquardt, D.W., 1970, "Generalized inverses, ridge regression, biased linear estimation, and nonlinear estimation", *Technometrics*, 12, 3, pp. 591–612.

Oliveira Jr., V. C., and V. C. F. Barbosa, 2013, 3-D radial gravity gradient inversion: *Geophysical Journal International*, 195, no. 2, 883–902.

Oliveira Jr., V. C., V. C. F. Barbosa, and J. B. C. Silva, 2011, Source geometry estimation using the mass excess criterion to constrain 3-D radial inversion of gravity data: *Geophysical Journal International*, 187, no. 2, 754–772.

Plouff, D., 1976, Gravity and magnetic fields of polygonal prisms and application to magnetic terrain corrections: *Geophysics*, 41, no. 4, 727–741.

Pratt, D. A., Foss, C. A., Shi, Z., Mann, S., White, A. S., Gidley, P. R., and McKenzie, K. B., 2005, ModelVision Pro, AutoMag Reference Manual Version 7.00, Encom Technology, 504 p.

Uieda, L., V. C. Oliveira Jr., and V. C. F. Barbosa, 2013, Modeling the earth with fatiando a terra: *Proceedings of the 12th Python in Science Conference*, 91–98.

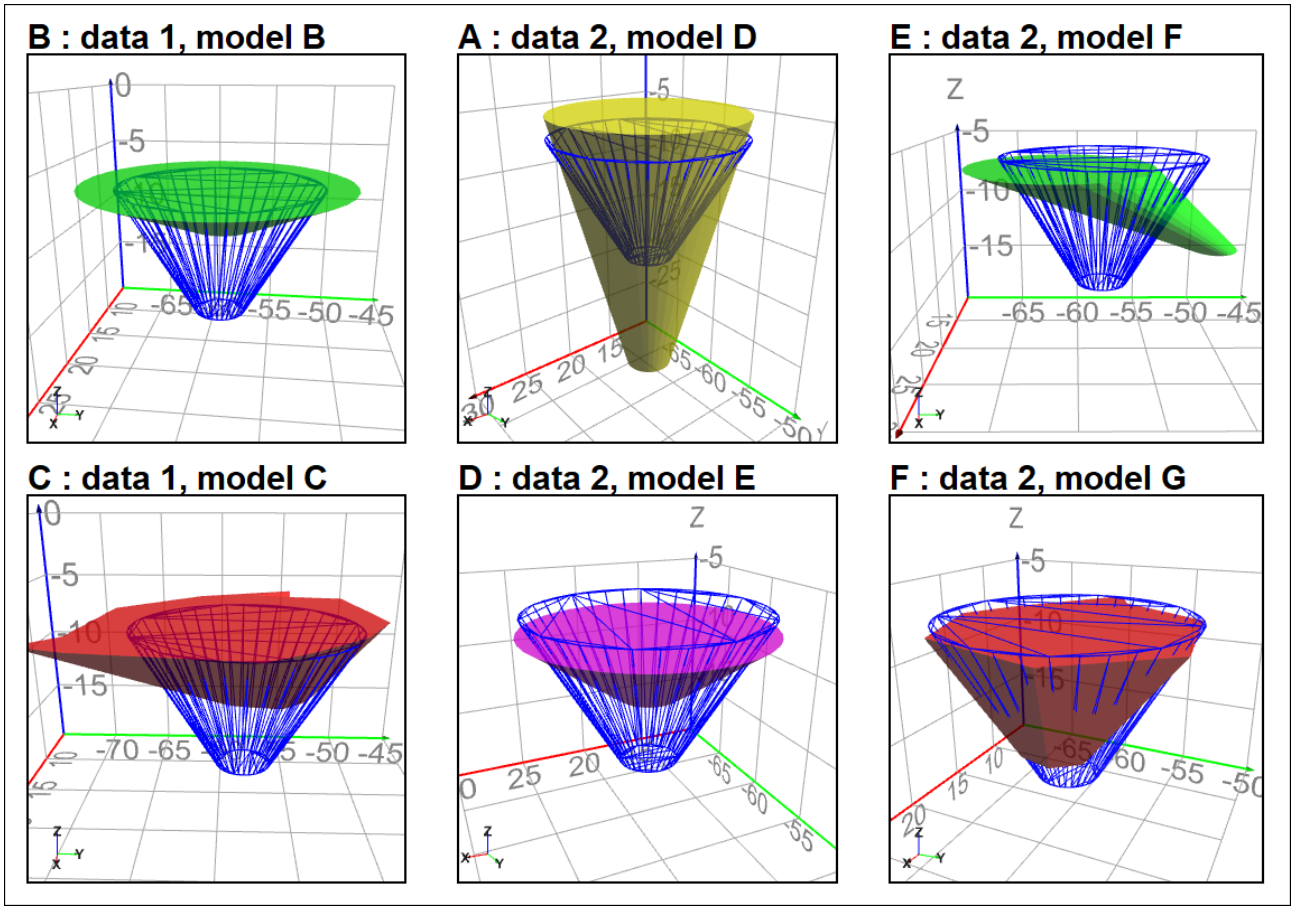

Figure 3. Known magnetization distribution Model A (blue wire-frame) and corresponding models B to G, inverted to match the measured data (data 1) and Model A computed data (data 2).

model	data	software	description	top_depth	top_area	susceptibility	depth_extent	volume	moment	data misfit
				cm	sq cm	SI	cm	cm^3	A.m^2	%
A	**1**	**MV**	**known geometry**	**6**	**154**	**0.2**	**9**	**579**	**0.0053**	**10.5**
B	1	MV	best plunging circular funnel	5.9 (-2%)	272 (+77%)	0.323 (+63%)	2.6 (-71%)	296 (-49%)	0.0044 (-17%)	9.2 (-12%)
C	1	MV	best plunging polygonal funnel	5.6 (-7%)	240 (+56%)	0.219 (+11%)	4.3 (-52%)	449 (-22%)	0.0045 (-15%)	5.3 (-50%)
D	2	MV	vertical circular funnel susc 50%	4.4 (-27%)	154 (0%)	0.1 fixed	20 (+122%)	1298 (+124%)	0.0059 (+11%)	1.8 (-70%)
E	2	MV	vertical circular funnel susc 200%	7 (+17%)	167 (+8%)	0.4 fixed	3.9 (-57%)	276 (-52%)	0.0050 (-5%)	0.6 (-94%)
F	2	MV	best plunging elliptical funnel	6.7 (+12%)	149 (-3%)	0.334 (+69%)	5.8 (-36%)	349 (-40%)	0.0053 (0%)	5 (-52%)
G	2	MV	best plunging polygonal funnel	6.6 (+10%)	157 (+2%)	0.283 (+43%)	5.9 (-34%)	402 (-31%)	0.0052 (-2%)	2.8 (-73%)
H	**1**	**RI**	**known geometry**	**6**	**141 (-8%)**	**0.2**	**10 (+11%)**	**597 (+3%)**	**0.0054 (+1%)**	**10 (-5%)**
I	1	RI	changing the depth to the top	6.5 (+8%)	150 (-2%)	0.2	8 (-11%)	680 (+17%)	0.0062 (+17%)	12.7 (+21%)
J	**2**	**RI**	**known geometry**	**6**	**134 (-12%)**	**0.2**	**12.4 (+37%)**	**612 (+5%)**	**0.0056 (+5%)**	**3.15 (-70%)**
K	2	RI	changing the depth to the top	6.5 (+8%)	125 (-19%)	0.2	10 (+89%)	599 (+3%)	0.0055 (-5%)	9.4 (-10%)

Table 1. Inversion model statistics with (in brackets) differences from the corresponding known geometry Model A statistic.

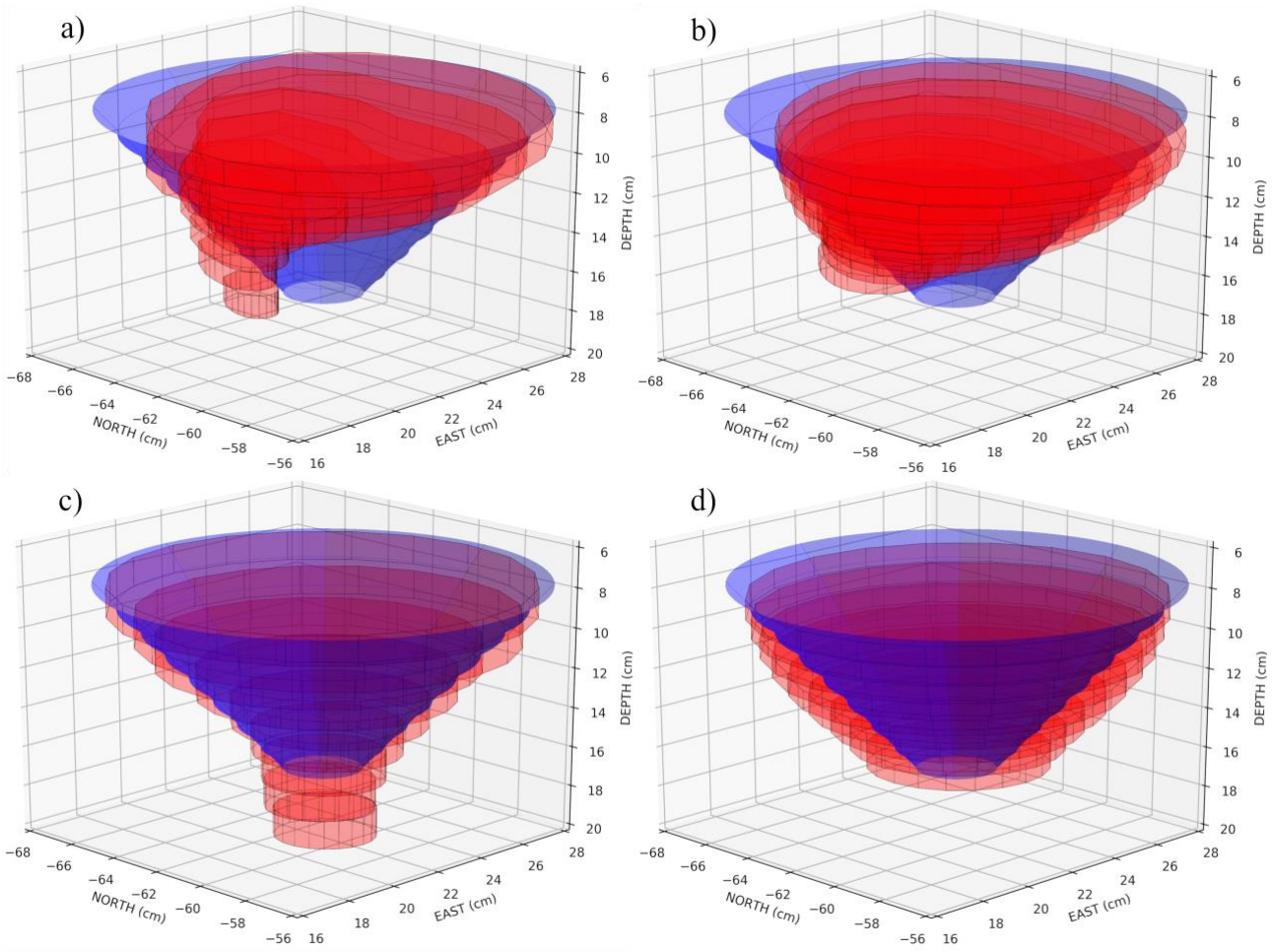

Figure 4: Inverse models using the new method compared to the known magnetization distribution Model A (blue surface). The red prisms in a) and b) are the H and I inversion models for the measured data (data 1). The red prisms in c) and d) are the J and K inversion models for the Model A computed data (data 2).